

Lithium aluminosilicate reinforced with carbon nanofiber and alumina for controlled-thermal-expansion materials

This article has been downloaded from IOPscience. Please scroll down to see the full text article.

2012 Sci. Technol. Adv. Mater. 13 015007

(<http://iopscience.iop.org/1468-6996/13/1/015007>)

View [the table of contents for this issue](#), or go to the [journal homepage](#) for more

Download details:

IP Address: 158.42.239.61

The article was downloaded on 10/02/2012 at 10:57

Please note that [terms and conditions apply](#).

Lithium aluminosilicate reinforced with carbon nanofiber and alumina for controlled-thermal-expansion materials

Amparo Borrell¹, Olga García-Moreno¹, Ramón Torrecillas¹,
Victoria García-Rocha² and Adolfo Fernández²

¹ Centro de Investigación en Nanomateriales y Nanotecnología (CINN) (Consejo Superior de Investigaciones Científicas—Universidad de Oviedo—Principado de Asturias), Parque Tecnológico de Asturias, 33428 Llanera (Asturias), Spain

² ITMA Materials Technology, Parque Tecnológico de Asturias, 33428 Llanera (Asturias), Spain

E-mail: a.borrell@cinn.es

Received 12 September 2011

Accepted for publication 11 December 2011

Published 9 February 2012

Online at stacks.iop.org/STAM/13/015007

Abstract

Materials with a very low or tailored thermal expansion have many applications ranging from cookware to the aerospace industry. Among others, lithium aluminosilicates (LAS) are the most studied family with low and negative thermal expansion coefficients. However, LAS materials are electrical insulators and have poor mechanical properties. Nanocomposites using LAS as a matrix are promising in many applications where special properties are achieved by the addition of one or two more phases. The main scope of this work is to study the sinterability of carbon nanofiber (CNFs)/LAS and CNFs/alumina/LAS nanocomposites, and to adjust the ratio among components for obtaining a near-zero or tailored thermal expansion. Spark plasma sintering of nanocomposites, consisting of commercial CNFs and alumina powders and an *ad hoc* synthesized β -eucryptite phase, is proposed as a solution to improving mechanical and electrical properties compared with the LAS ceramics obtained under the same conditions. X-ray diffraction results on phase compositions and microstructure are discussed together with dilatometry data obtained in a wide temperature range (-150 to 450 °C). The use of a ceramic LAS phase makes it possible to design a nanocomposite with a very low or tailored thermal expansion coefficient and exceptional electrical and mechanical properties.

Keywords: ceramic-matrix composites, carbon nanofibers, spark plasma sintering, mechanical properties, coefficient of thermal expansion

1. Introduction

A very low or controlled thermal-expansion property is required to achieve high precision in modern industries, such as optics, microelectronics and energy transformation, to reduce measurement errors due to thermal deformation [1, 2]. The relevant materials are of great interest because their coefficient of thermal expansion (CTE) can be controlled by adjusting their chemical composition. While most materials expand upon heating, some contract [3, 4]; in particular, cordierite, aluminum titanate, zirconium tungstate, β -eucryptite and β -spodumene are well known for their low or negative thermal expansion coefficient [3, 5–7].

The development of materials with near-zero or controlled CTE in a wide temperature range is a difficult task. The lithium aluminosilicate family (LAS) is the most studied system composed of materials with very low CTE. Glass-ceramics based on the LAS system are currently used in components with low thermal expansion. However, the temperature range where CTE is close to zero is very narrow, and the mechanical properties of these materials are poor, particularly at elevated temperatures. Consequently, ceramic materials without glass components are a very attractive alternative. Eucryptite and spodumene are the most used and studied phases exhibiting these characteristics, with β -eucryptite having the largest negative CTE in the

LAS system [8, 9]. These materials have low-temperature invariant points, and therefore are difficult to sinter into dense ceramic bodies owing to the easy formation of a vitreous phase [10–12]. For this reason, they are usually employed as glass-ceramic composites [4, 13–15]. Since the ceramic materials obtained in this system by pressureless sintering have poor mechanical properties (in particular, low Young's moduli), a possible solution is to apply unconventional sintering methods. Spark plasma sintering (SPS) is one of such methods allowing to obtain relatively dense materials with very low amounts of a glassy phase [16]. This technique is proposed in this work as a possible solution to producing LAS ceramics with improved mechanical properties.

SPS opens a wide variety of possibilities in the design of nanocomposites as it can produce dense composites and allows grain growth control during sintering. Previous studies revealed a necessity for the control of the sinterability of LAS composites and for the design of compositions with a low and tunable CTE [17]. The latter goal can be achieved by mixing β -eucryptite with various positive-thermal-expansion-coefficient materials.

New materials with controlled CTE (and other properties) can be obtained by adjusting the volume fractions of different phases and sintering them by SPS at various temperatures. One of the main limitations of LAS-based low-CTE materials is their insulating nature. Shaping these materials would be facilitated if they could be processed by electrical discharge machining (EDM), which requires electrical resistivity below $100 \Omega \text{ cm}$. This property is important because EDM allows the production of samples with complex geometries and very good surface finishing and can be applied to materials with a wide range of hardness. EDM offers several other advantages over traditional machining methods, such as low processing costs.

In this work, carbon nanofibers (CNFs) were used as the conductive phase and alumina as the mechanical reinforcement in the novel CNFs/LAS and CNFs/alumina/LAS nanocomposites, and the thermal expansion, mechanical and electrical properties of these composites were evaluated.

2. Experimental procedures

2.1. Materials

A β -eucryptite solid solution (hereafter referred to as LAS) with the chemical composition $1 : 1.01 : 3.11 \text{ Li}_2\text{O} : \text{Al}_2\text{O}_3 : \text{SiO}_2$ was synthesized as described in our previous work [18]. The resulting powder was composed of β -eucryptite with traces of quartz and spodumene and had an average grain size of $1 \mu\text{m}$. Its CTE properties were reported in [18] and used in designing composites with low, tunable expansion in a wide temperature range.

The raw material used in this study as a second phase was commercial CNFs with an average outer diameter of $20\text{--}80 \text{ nm}$ and a length exceeding $30 \mu\text{m}$. These CNFs were grown from a vapor phase [19] using a nickel solution (6–8%) as a floating catalyst and supplied by Group Antolín Engineering (Burgos, Spain). The third phase was $\alpha\text{-Al}_2\text{O}_3$

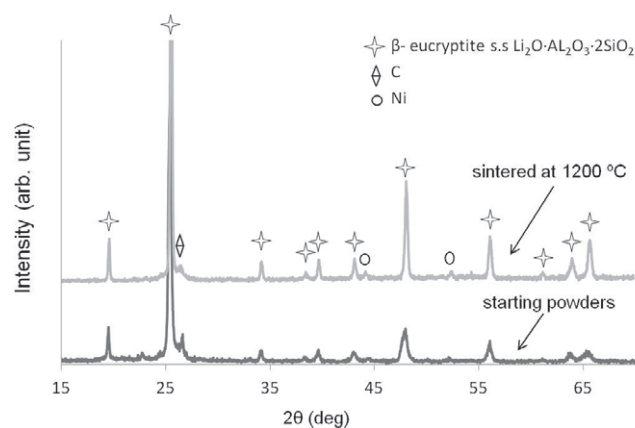


Figure 1. XRD patterns of LAS/20 vol.% CNFs starting powders and composite processed by SPS at $1200 \text{ }^\circ\text{C}$.

nanopowder (Taimei TM-DAR Chemicals Co. Ltd, Japan) with an average particle size of 160 nm and a purity of 99.99%. The powder mixtures were dispersed in ethanol (Panreac Quimica) and processed with a high-energy attrition mill (Union Process, USA) for 1 h at 400 rpm, using alumina balls of 2 mm diameter. After milling, the resultant homogeneous slurries were dried at $60 \text{ }^\circ\text{C}$ and sieved through a $60 \mu\text{m}$ mesh. The final compositions were LAS/20 vol.% CNFs and LAS/40 vol.% Al_2O_3 /20 vol.% CNFs.

2.2. Sintering and characterization

The powder samples were uniaxially pressed at 30 MPa and sintered using an SPS apparatus HP D 25/1 from FCT Systeme (Rauenstein, Germany) in a vacuum of 0.1 mbar . The powders were placed in a graphite die with an inner diameter of 20 mm and sintered at different temperatures for 1 min. The maximum applied pressure was 50 MPa , and a heating rate of $100 \text{ }^\circ\text{C min}^{-1}$ was used. The resulting materials were characterized for theoretical density, for apparent or relative density using the Archimedes method, and for absolute density using He pycnometry. The final density of the composites was calculated using the rule of the mixture and densities of 3.98 g cm^{-3} for alumina, 2.01 g cm^{-3} for CNFs and 2.40 g cm^{-3} for LAS. The fracture strength was measured via biaxial testing, employing the equations of Kirstein and Woolley [20], Vitman and Pukh [21], and the standard specification ASTM F394-78 [22]. Five samples were tested for each composition. All the tests were performed at room temperature using a universal machine Instron (Model 8562) with a cross-head displacement speed of 0.002 mm s^{-1} .

The samples for fracture toughness analysis were polished to $1 \mu\text{m}$ roughness using a RotoPol-31 (Struers) polisher and diamond paste. The fracture toughness (K_{IC}) was determined using the indentation technique (Buehler, model Micromet 5103) with a conventional diamond pyramid indenter loaded to 98 N . The length of the cracks of each indentation was measured under an optical microscope. Ten diagonals were evaluated for each composition using the Evans–Charles equation [23].

Fracture surfaces and polished cross sections of sintered samples were imaged by scanning electron microscopy

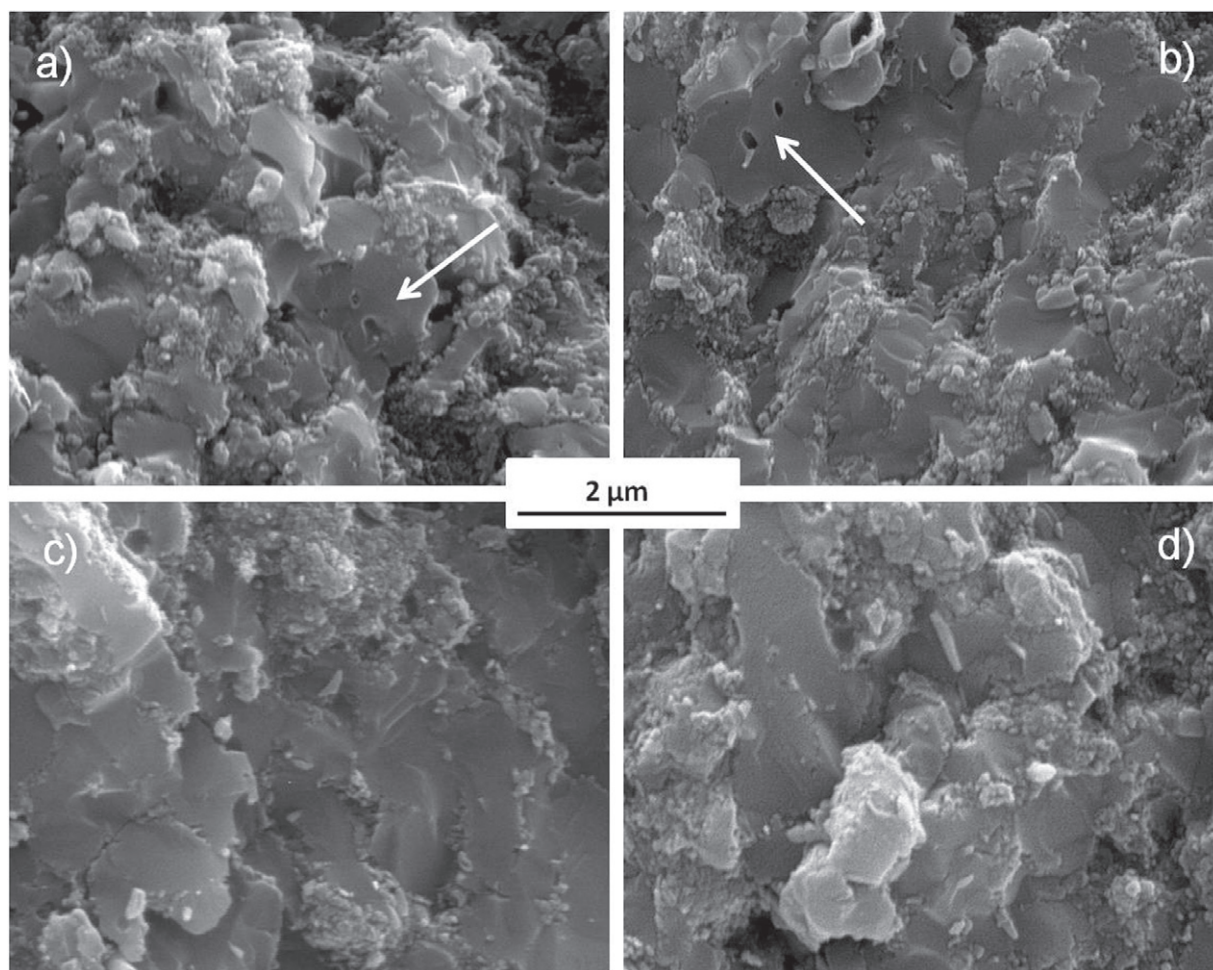


Figure 2. SEM images of fracture surfaces of LAS/20 vol.% CNFs composites sintered at (a) 1000, (b) 1100, (c) 1150 and (d) 1200 °C.

(SEM, Zeiss DSM 950). The nanocomposite powders were characterized by x-ray diffraction (XRD), in the Bragg-Brentano geometry, using $\text{CuK}\alpha$ radiation at 40 kV and 30 mA ($\lambda = 0.154$ 18 nm) and a Siemens D5000 diffractometer equipped with a tube monochromator. The measurements were performed in the angular range of 15–70° with a step of 0.02° and integration time of 0.3 s. The electrical resistivity of monolithic and composite materials was determined according to the ASTM C611 standard. The specimens were placed between two sheets of copper separated by 9.55 mm and connected to a power supply, and the current was set at 0.5 A. The coefficient of thermal expansion was measured with a dilatometer (Netzsch DIL402C). The dilatometer was coupled to a liquid nitrogen Dewar, enabling measurements between –150 and 450 °C.

3. Results and discussion

3.1. Composites LAS/20 vol.% CNFs

Figure 1 shows the XRD patterns of the starting powder mixture and a composite sintered at 1200 °C, revealing that the β -eucryptite phase is present both the starting powders and the sintered composite. No reaction occurred between the LAS phase and CNFs, with β -eucryptite being the dominant

crystalline phase of the LAS/CNFs composites. Negligible amounts of glassy phase were formed. Ni peaks were detected in the diffractogram and attributed to the catalyst that was used to grow the CNFs [19]. Glass phases were observed neither in the XRD diffractogram nor in the SEM images, which are described below (figure 2).

Samples sintered at 1150 and 1200 °C (panels c and d) have negligible porosity, while pores are observed in samples obtained at lower temperatures (1000 and 1100 °C—panels a and b, respectively), as marked by arrows. The pores are located inside LAS grains and between phases. No glassy phase is observed, confirming the XRD results. CNFs are homogeneously distributed around the LAS grains, preventing their growth, and resulting in a similar grain size ($\sim 1 \mu\text{m}$) of the LAS phase for all the sintering temperatures tested. As a result, even after adding 20 vol.% carbon phase, which is relatively weak in comparison with the ceramic matrix, the effect of microstructure control leads to an improvement in the mechanical properties of the composite.

Table 1 lists the relative density, fracture strength, fracture toughness, electrical resistivity and thermal expansion coefficient of the LAS/20 vol.% CNFs materials sintered at different temperatures by SPS. The density and fracture strength significantly increase with sintering temperature, and the relative density of the composite sintered at 1200 °C is

Table 1. Relative densities, fracture strength, fracture toughness, electrical resistivity and thermal expansion coefficient of LAS + 20 vol.% CNFs composites sintered at different temperatures by SPS.

Sintering temperature (°C)	Relative density (%)	Fracture strength (MPa)	Fracture Toughness (MPa m ^{1/2})	Electrical resistivity (Ω cm)	CTE -150 to 450 °C (×10 ⁻⁶ K ⁻¹)	CTE 25 to 450 °C (×10 ⁻⁶ K ⁻¹)
1000	94.6	86.3 ± 2.2	—	1.2 ± 0.05	—	—
1100	96.3	95.2 ± 4.3	—	1.1 ± 0.05	-0.75 ± 0.05	-0.28 ± 0.05
1150	98.2	125.1 ± 3.5	2.02 ± 0.08	1.0 ± 0.05	-0.79 ± 0.05	-0.33 ± 0.05
1200	99.7	164.5 ± 5.4	2.28 ± 0.10	1.1 ± 0.05	-0.69 ± 0.05	-0.32 ± 0.05
LAS 1200	98.8	140.0 ± 4.9	1.68 ± 0.05	10 ⁸ ± 0.05	-0.9 ± 0.05	-0.45 ± 0.05

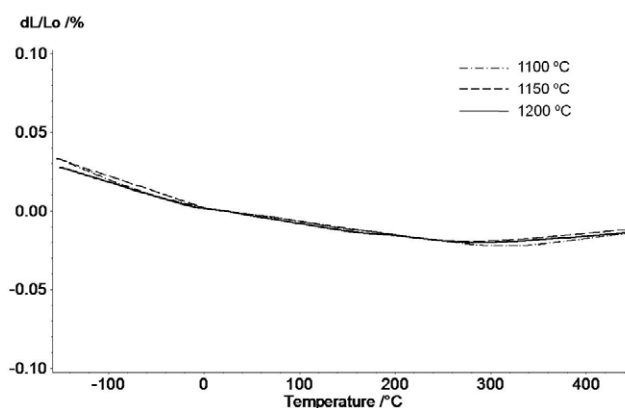
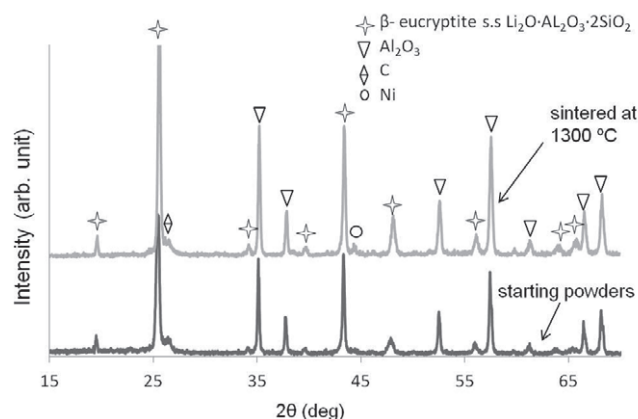
99.7%. Thus, highly dense composites were prepared, the relatively low sintering temperatures hindered the formation of a glassy phase in the LAS system, and strengths increased as the composite density reached the theoretical density. Moreover, the addition of carbon nanofibers increased the fracture toughness—although the absolute toughness is moderate, it was improved by more than 30% as compared with that of the *ad hoc* synthesized β -eucryptite phase sintered by SPS at 1200 °C.

Considering that the fracture strength of vitreous LAS is 10–15 MPa [4], the fracture strength of the composite prepared at 1200 °C would be considerably lower if a glass phase was formed. The combination of heat and pressure applied by the SPS process and the dramatic reduction in cycle time allows densification without glass phase formation. Note the crucial role of sintering temperature: an increase of only 50 °C results in a 30% increase in the fracture strength.

The electrical resistivity of LAS/CNFs composites is very low compared with that of LAS (108 Ω cm); the values were similar under all the conditions tested and only depended on the composition of the material. The role of carbon nanofibers in SPS is essential, not only for the properties of the obtained material, but also for the sintering process itself. As the sample is heated by passing electric current through the graphite die, if the sample is an insulator, a temperature gradient is formed between the outer (in contact with the die wall) and inner parts of the sample. The presence of CNFs results in a homogeneous distribution of electric current through the sample avoiding or noticeably reducing temperature gradients. This control is particularly important for the materials studied in this work, wherein a temperature gradient could lead to glass formation in the hotter parts of a sample without complete densification of the colder regions.

The thermal expansion coefficients of the LAS/20 vol.% CNFs sintered samples with higher densities are listed in table 1. Figure 3 shows the elongation versus temperature curves for samples sintered at 1100, 1150 and 1200 °C revealing very low and weakly temperature dependent values.

The dilatometric curves of these composites are very similar. Therefore, the sintering temperature and small differences in density do not significantly affect the CTE value. The CTE in the LAS/20 vol.% CNFs system is almost constant between -150 and 450 °C. This temperature range is considerably wider than those scanned for most low-CTE materials (~50 °C). Thus, the combination of two phases with positive and negative CTE resulted in a composite exhibiting a low CTE over a wide temperature range. In this composite,

**Figure 3.** Elongation versus temperature of LAS/20 vol.% CNFs sintered samples.**Figure 4.** XRD patterns of LAS/40 vol.% Al₂O₃/20 vol.% CNFs starting powders and composite sintered at 1300 °C.

carbon nanofibers provide electrical conductivity, reduce total weight and allow the adjustment of the CTE value. These characteristics are required for applications such as space mirror blanks and other aerospace products.

3.2. Composites LAS/40 vol.% Al₂O₃/20 vol.% CNFs

Figure 4 shows XRD patterns of the LAS/40 vol.% Al₂O₃/20 vol.% CNFs starting powder mixture and the composite sintered at 1300 °C. They reveal that the main crystalline component is β -eucryptite, with no other LAS phases formed, and it is accompanied by α -alumina. Recent studies have corroborated the compatibility between alumina and the LAS composition studied in this work [24]. The stability

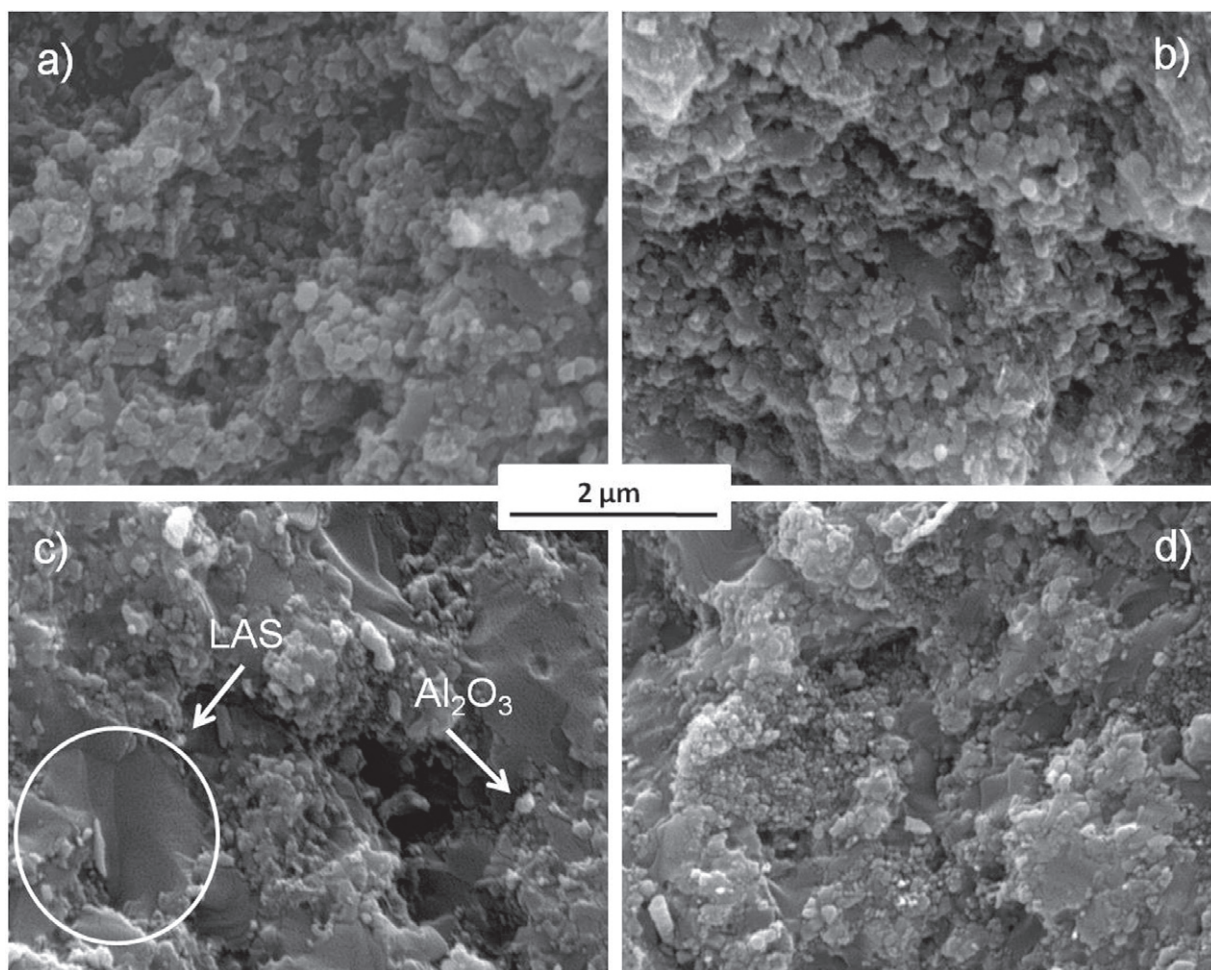


Figure 5. SEM images of fracture surfaces of LAS/40 vol.% Al_2O_3 /20 vol.% CNFs composites sintered at (a) 1100, (b) 1200, (c) 1250 and (d) 1300 °C.

of the phases during the sintering process (SPS) is essential for controlling the composition of the final material, and, therefore, its thermal expansion coefficient.

Figure 5 shows fracture surfaces of LAS/40 vol.% Al_2O_3 /20 vol.% CNFs nanocomposites sintered at different temperatures. The porosity of the samples sintered at low temperatures of 1100 and 1200 °C, which is higher than 10%, can be clearly observed in images a and b, respectively. The spark plasma sintering process has not been completed, as can be inferred from the rounded shape of the grains, which explains the low density of the samples. Images c and d indicate the full densification of the samples sintered at 1250 and 1300 °C, respectively. Image c shows that the grain size of LAS is about 1–1.5 μm , while that of alumina is in the nanometer range. As in the CNFs/LAS composites, carbon nanofibers are homogeneously distributed in the composite.

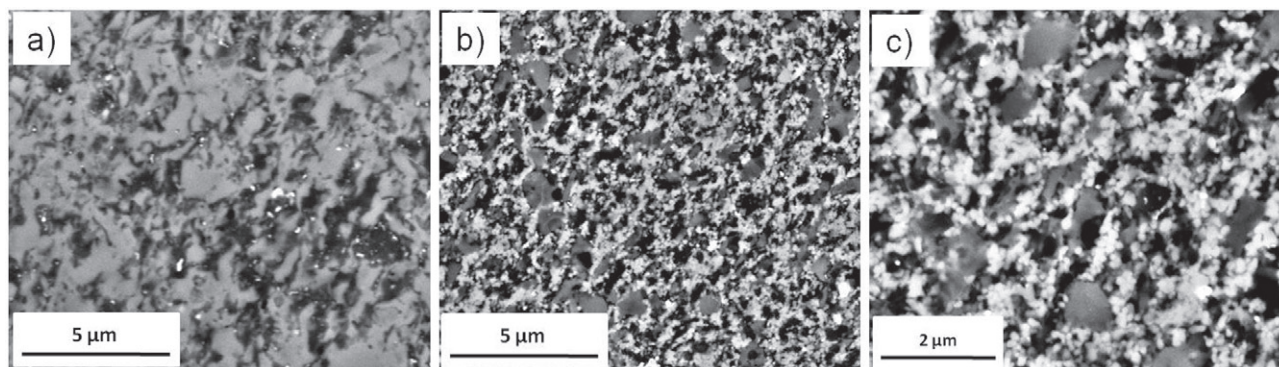
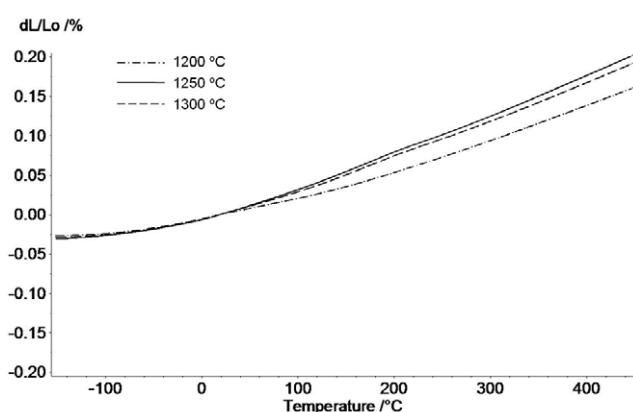
The incorporation of alumina as a third phase provides an interesting opportunity to optimize some properties of LAS-based materials, as dispersed alumina nanoparticles contribute to the CTE balance and improve the mechanical properties of a composite [24]. Table 2 shows the relative density, fracture strength, fracture toughness and electrical resistivity of the LAS/40 vol.% Al_2O_3 /20 vol.% CNFs material sintered at different temperatures using SPS. The

density and fracture strength significantly increased with temperature, particularly from 1200 to 1250 °C, when high densification is achieved. The comparison of fracture toughness values reveals the additive effect of alumina and carbon nanofibers on the LAS matrix: the toughness of the LAS/ Al_2O_3 /CNFs composite is more than twice higher than that of pure LAS, and is noticeably higher than that of the LAS/CNFs composite. Dense monolithic alumina can be obtained by SPS at relatively high temperatures of 1250–1300 °C. Therefore, the presence of 40 vol.% alumina raises the temperature required to reach densities higher than 99% of theoretical values in LAS/ Al_2O_3 /CNFs composites. As for electrical resistivity values, they are comparable in LAS/ Al_2O_3 /CNFs and LAS/CNFs materials, as expected. The electrical resistivity only depends on the CNFs content.

To complete the microstructural characterization of these materials, SEM images of the polished LAS/20 vol.% CNFs composite sintered at 1200 °C and the LAS/40 vol.% Al_2O_3 /20 vol.% CNFs composite sintered at 1250 °C are shown in figure 6. LAS, alumina and CNFs components are observed as gray, white and black features, respectively. The addition of reinforcing components allowed us the control of the LAS grain size, particularly in the three-phase composite. Thanks to the microstructure control and homogeneous

Table 2. Relative densities, fracture strength, fracture toughness, electrical resistivity and thermal expansion coefficient of LAS + 40 vol.% Al₂O₃ + 20 vol.% CNFs composites sintered at different temperatures by SPS.

Sintering temperature (°C)	Relative density (%)	Fracture strength (MPa)	Fracture toughness (MPa m ^{1/2})	Electrical resistivity (Ω cm)	CTE -150 to 450 °C (× 10 ⁻⁶) K ⁻¹	CTE 25 to 450 °C (× 10 ⁻⁶) K ⁻¹
1100	75.5	44.0 ± 2.6	—	2.6 ± 0.05	—	—
1200	87.6	142.3 ± 3.7	2.37 ± 0.15	2.2 ± 0.05	3.13 ± 0.05	3.74 ± 0.05
1250	98.8	308.4 ± 4.2	3.66 ± 0.20	2.1 ± 0.05	3.88 ± 0.05	4.71 ± 0.05
1300	98.7	306.3 ± 3.9	3.64 ± 0.20	2.1 ± 0.05	3.68 ± 0.05	4.47 ± 0.05

**Figure 6.** SEM images of polished surfaces of LAS/20 vol.% CNFs sample sintered at 1200 °C (a) and LAS/40 vol.% Al₂O₃/20 vol.% CNFs sample sintered at 1250 °C (b, c).**Figure 7.** Elongation versus temperature of LAS/40 vol.% Al₂O₃/20 vol.% CNFs sintered samples.

distribution of the components in the bulk composites, their mechanical properties have been improved.

Dilatometric studies of the LAS/40 vol.% Al₂O₃/20 vol.% CNFs sintered samples were performed in the temperature range of -150 to 450 °C. The measured elongation versus temperature curves are shown in figure 7 and the thermal expansion coefficients are listed in table 2.

The CTE values in table 2 are positive, as expected from the composition, which was chosen to explore the effect of alumina addition rather than optimize the CTE value. The curves of figure 7 approximately follow the rule of mixtures, taking into account the individual CTE values for alumina, CNFs and LAS as (6–7, 4–5 and 0.8) × 10⁻⁶ K⁻¹, respectively. In this composite, the sintering temperature affects the CTE via density. In particular, the CTE value decreases when the sintering temperature is increased from

1250 to 1300 °C which can be attributed to the change in the CTE value of the LAS component when it is sintered at relatively high temperatures. This effect has been studied for LAS materials prepared by pressureless sintering, and a similar effect can occur in SPS [18]. The change in the CTE value with temperature cannot be related to the effect of grain size or microcracking as proposed in [25, 26], as such no increase in grain size was observed in our SPS samples.

The results of this work prove the possibility of preparing composites of LAS, Al₂O₃ and CNFs with a controlled phase composition. This achievement allows us the design of materials with interesting properties, such as significant electrical conductivity, high fracture strength and controlled coefficient of thermal expansion: increasing the amount of CNFs and Al₂O₃ fraction will improve the electrical conductivity and mechanical properties, respectively, while the content of LAS will determine the CTE value.

4. Conclusions

Dense LAS/CNFs and LAS/CNFs/Al₂O₃ composites were fabricated by spark plasma sintering at relatively low temperatures. They exhibited superior mechanical properties and higher electrical conductivity than monolithic LAS materials. The CNFs component resulted in the homogeneous distribution of the electrical current and thereby hindered temperature gradients that can occur within the sample during sintering. As a result, a fully densified material was obtained without melting. The thermal expansion coefficients of these materials make them suitable for use in components with high dimensional stability. High fracture strength (>300 MPa) was achieved in the LAS/CNFs/Al₂O₃ system. The non reactivity

of LAS with carbon nanofibers and/or Al₂O₃ facilitates tailoring of the composite properties.

Acknowledgments

This work was financially supported by the National Plan Projects MAT2006-01783 and MAT2007-30989-E and the Regional Project FICYT PC07-021. A Borrell thanks the Spanish Ministry of Science and Innovation for her research grant BES2007-15033. O García-Moreno is working for CSIC under a JAE-Doc contract co-funded by the ESF.

References

- [1] Yang X, Cheng X, Yan X, Yang J, Fu T and Qiu J 2007 *Compos. Sci. Technol.* **67** 1167
- [2] Namba Y, Takehara H and Nagano Y 2001 *CIRP Ann. Manuf. Technol.* **50** 239
- [3] Chen J C, Huang G C, Hu C and Weng J P 2003 *Scr. Mater.* **49** 261
- [4] Bach H 1995 *Low Thermal Expansion Glass Ceramics* (Berlin: Springer) p 223
- [5] Kenneth M 1962 *Am. Ceram. Soc. Bull.* **41** 783
- [6] García-Verdúch A and Moya J S 1972 *Proc. Int. Clay Conf.* pp 131–9
- [7] Moya J S, García-Verdúch A and Hortal M 1974 *Trans. J. Br. Ceram. Soc.* **73** 177
- [8] Abdel-Fattah W I and Abdellah R 1997 *Ceram. Int.* **23** 463
- [9] Sheu G J, Chen J C, Shiu J Y and Hu C 2005 *Scr. Mater.* **53** 577
- [10] Roy R, Agrawal D K and Mckinstry H A 1989 *Annu. Rev. Mater. Sci.* **19** 59
- [11] Chen J C and Sheu G J 2004 *US Patent* 6764565B2
- [12] Mandal S, Chakrabarti S, Das S and Ghatak S 2004 *Ceram. Int.* **30** 2147
- [13] Barbieri L, Leonelli C, Manfredini T, Siligardi C, Corradi A B, Mustarelli P and Tomasi C 1997 *J. Am. Ceram. Soc.* **80** 3077
- [14] Riello P, Bucella S, Zamengo L, Anselmi-Tamburini U, Francini R, Pietrantonio S and Munir Z A 2006 *J. Eur. Ceram. Soc.* **26** 3301
- [15] Tkalčec E, Šeniija D, Dondur V and Petranović N 1992 *J. Am. Ceram. Soc.* **75** 1958
- [16] García-Moreno O, Fernández A and Torrecillas R 2011 *Ceram. Int.* **37** 1079
- [17] García-Moreno O, Fernández A and Torrecillas R 2010 *J. Eur. Ceram. Soc.* **30** 3219
- [18] García-Moreno O, Fernández A, Khainakov S and Torrecillas R 2010 *Scr. Mater.* **63** 170
- [19] Martín-Gullón I, Vera-Agulló J, Conesa J, González J L and Merino C 2006 *Carbon* **44** 1572
- [20] Kirstein A F and Woolley R M J 1967 *Res. Natl Bur. Stand. C* **71** 1
- [21] Vitman F F and Pukh V P 1963 *Zavod Lab.* **29** 863
- [22] ASTM Standard F394-78 1996 *Annual Book of Standards* vol **15** (Philadelphia, PA: American Society for Testing and Materials) p 466
- [23] Evans A G and Charles E A 1976 *J. Am. Ceram. Soc.* **59** 371
- [24] García-Moreno O, Borrell A, Bittmann B, Fernández A and Torrecillas R 2011 *J. Eur. Ceram. Soc.* **31** 1641
- [25] Ogiwara T, Noda Y, Shoji K and Kimura O 2011 *J. Am. Ceram. Soc.* **94** 1427
- [26] Pelletant A, Reveron H, Chevalier J, Fantozzi G, Blanchard L, Guinot F and Falzon F 2011 *Mater. Lett.* at press (uncorrected proof available, online 3 August 2011)